multimedia

Green fluorescent protein (GFP) tagged to the cytoplasmic tail of αIIb or β3 allows the expression of a fully functional integrin αIIbβ3: effect of $\beta3_{GFP}$ on αIIbβ3 ligand binding

Sébastien PLANÇON, Marie-Christine MOREL-KOPP, Elisabeth SCHAFFNER-RECKINGER, Ping CHEN and Nelly KIEFFER[1]

Laboratoire Franco-Luxembourgeois de Recherche Biomédicale (CNRS and CRP-Santé), Centre Universitaire, L-1511 Luxembourg, Grand-Duchy of Luxembourg

Using green fluorescent protein (GFP) as an autofluorescent tag, we report the first successful visualization of a β3 integrin in a living cell. GFP fused in frame to the cytoplasmic tail of either αIIb or β3 allowed normal expression, heterodimerization, processing and surface exposure of $\alpha IIb_{GFP}\beta3$ and $\alpha IIb\beta3_{GFP}$ receptors in Chinese hamster ovary (CHO) cells. Direct microscopic observation of the autofluorescent cells in suspension following antibody-induced αIIbβ3 capping revealed an intense autofluorescent cap corresponding to unlabelled immunoclustered GFP-tagged αIIbβ3. GFP-tagged αIIbβ3 receptors mediated fibrinogen-dependent cell adhesion, were readily detectable in focal adhesions of unstained living cells and triggered $p125^{FAK}$ tyrosine phosphorylation similar to wild-type αIIbβ3 (where FAK corresponds to focal adhesion kinase). However, GFP tagged to β3, but not to αIIb, induced spontaneous CHO cell aggregation in the presence of soluble fibrinogen, as well as binding of the fibrinogen mimetic monoclonal antibody PAC1 in the absence of αIIbβ3 receptor activation. Time-lapse imaging of living transfectants revealed a characteristic redistribution of GFP-tagged αIIbβ3 during the early stages of cell attachment and spreading, starting with αIIbβ3 clustering at the rim of the cell contact area, that gradually overlapped with the boundary of the attached cell, and, with the onset of cell spreading, to a reorganization of αIIbβ3 in focal adhesions. Taken together, our results demonstrate that (1) fusion of GFP to the cytoplasmic tail of either αIIb or β3 integrin subunits allows normal cell surface expression of a functional receptor, and (2) structural modification of the β3 integrin cytoplasmic tail, rather than the αIIb subunit, plays a major role in αIIbβ3 affinity modulation. With the successful direct visualization of functional αIIbβ3 receptors in living cells, the generation of autofluorescent integrins in transgenic animals will become possible, allowing new approaches to study the dynamics of integrin functions.

Key words: fibrinogen receptor, integrin affinity modulation, integrin signalling, platelet GPIIb-IIIa, vitronectin receptor.

INTRODUCTION

With the development of green fluorescent protein (GFP) as an autofluorescent reporter protein, studies on the subcellular localization and dynamics of specific components within the living cell have been made possible [1]. GFP fused in frame with a large number of genes encoding proteins of interest has allowed the successful visualization of the dynamic properties of cellular organelles, the mitotic apparatus, cytoskeletal elements, protein trafficking and secretion events (reviewed in [2]). To date, however, only a few reports exist on the use of GFP as an autofluorescent marker of cell adhesion receptors [3–5], most probably due to the potential hindrance of the tagged GFP in receptor–ligand binding or intracellular signalling processes. To circumvent this drawback, alternative approaches have been developed, such as the generation of an autofluorescent chimaeric protein with an extracellular GFP fused to the transmembrane and cytoplasmic tail of an integrin β1 subunit, allowing co-localization of this GFP–β1 chimaera in focal adhesion plaques [6]. However, GFP–β1 fusion proteins do not support integrin–extracellular ligand interactions and therefore cannot be used to explore the dynamics of integrin functions in living cells.

Integrins are subject to rapid regulation of their ligand-binding capacities, a process known as inside-out signalling. The platelet fibrinogen receptor, integrin αIIbβ3, serves as a prototype for such regulation, since fibrinogen binding to αIIbβ3 only occurs following platelet activation [7]. Although the intracellular signalling pathways underlying this activation process are still incompletely characterized, there is convincing evidence that the high affinity state of αIIbβ3 is brought about by a conformational change of the receptor, allowing *de novo* exposure of a functional ligand-binding pocket [8]. Integrin cytoplasmic tails appear to be key effectors in this process as they have been shown to become phosphorylated and to interact with intracellular regulatory proteins [9,10]. In the present paper we describe the biochemical characterization and functional properties of the first autofluorescent intact β3 integrin, the GFP-tagged platelet fibrinogen receptor αIIbβ3. By fusing GFP to the cytoplasmic tail of β3, we expected a dominant negative effect of the GFP tag on β3 integrin receptor function. Surprisingly, however, the relatively large size of GFP did not interfere with integrin–cytoskeleton interactions or receptor signalling. In contrast, fusion of GFP to β3, but not to αIIb, induced a structural modification of the cytoplasmic tail of β3 allowing soluble fibrinogen binding and Chinese hamster ovary (CHO) cell aggregation. Using time-lapse imaging, a characteristic redistribution of αIIbβ3 was observed during the early stages of cell attachment, followed by eventual αIIbβ3 clustering in focal adhesions at the onset of cell spreading. With the demonstration that GFP tagged to the cytoplasmic tail of αIIb does not modify αIIbβ3 receptor function, the production of fully functional autofluorescent integrins in transgenic animals will become possible, allowing direct *in vivo* observation of the involvement of integrins at various stages of animal

Abbreviations used: 7-AAD, 7-amino-actinomycin D; CHO, Chinese hamster ovary; DABCO, 1,4-diazadicyclo[2.2.2]octane; DTT, dithiothreitol; FAK, focal adhesion kinase; GFP, green fluorescence protein; IMDM, Iscove's modified Dulbecco's medium; mAb, monoclonal antibody; wt, wild-type.

[1] To whom correspondence should be addressed (e-mail kieffer@cu.lu).

development, as well as in pathological conditions, such as inflammation, thrombosis, neoangiogenesis and tumour cell metastasis.

MATERIALS AND METHODS

Antibodies and reagents

The following monoclonal antibodies (mAbs) were used: P37 (anti-β3) was provided by Dr J. Gonzalez-Rodriguez (Instituto de Quimica Fisica, Madrid, Spain); S1.3 (anti-αIIb) and 4D10G3 (anti-β3) were provided by Dr D. Phillips (COR Therapeutics, South San Francisco, CA, U.S.A.); Pl2-46 and Pl2-73, two complex-specific anti-αIIbβ3 mAbs, were provided by Dr C. Kaplan (Institut National de la Transfusion Sanguine, Paris, France); 23C6 (anti-αvβ3) was provided by Dr M. Horton (Bone and Mineral Centre, The Middlesex Hospital, London, U.K.); and D3, provided by Dr L. Jennings (The University of Tennessee, Memphis, TN, U.S.A.). The blocking anti-αvβ3 mAb LM609, interacting with human αvβ3 and chimaeric $\alpha v_{(hamster)}\beta 3_{(human)}$, was obtained from Chemicon International (Temecula, CA, U.S.A.). The blocking hamster anti-α5β1 mAb PB1 was purchased from Developmental Studies Hybridoma Bank (Iowa City, IA, U.S.A.). The anti-phosphotyrosine PY-20 and anti-[focal adhesion kinase (FAK)] mAbs were purchased from Transduction Laboratories (Lexington, KY, U.S.A.), and the fibrinogen mimetic PAC1 (anti-αIIbβ3) was obtained from Becton Dickinson (San Jose, CA, U.S.A.). The polyclonal anti-FAK antibody was purchased from Santa Cruz Biotechnology (Santa Cruz, CA, U.S.A.), and the polyclonal anti-GFP antibody was obtained from ClonTech Laboratories (Palo Alto, CA, U.S.A.). R-phycoerythrin-conjugated goat anti-mouse IgM and IgG, FITC-conjugated goat anti-rabbit IgG, and rhodamine-conjugated goat anti-mouse IgG were purchased from Jackson Immunoresearch Laboratories (West Grove, PA, U.S.A.). Peroxidase-conjugated sheep anti-mouse or donkey anti-rabbit IgGs were obtained from Amersham Pharmacia Biotech (Roosendael, The Netherlands). Human fibrinogen was obtained from Calbiochem (San Diego, CA, U.S.A.), and human fibronectin, RGDS peptide and BSA (fraction V) were purchased from Sigma (Bornem, Belgium). 7-Amino-actinomycin D (7-AAD) and tetramethylrhodamine β-isothiocyanate ('TRITC')-conjugated phalloidin were obtained from Molecular Probes (Leiden, The Netherlands).

Plasmid constructs

The expression vector pEGFP-N1 (ClonTech Laboratories) was used to generate the αIIb_{GFP} and $\beta 3_{GFP}$ fusion proteins. The full-length αIIb cDNA (kindly provided by Dr D. Phillips) was excised from the pcDNA3.1/Zeo(3.1) vector by digestion with *Xba*I (5′) and *Hin*dIII (3′), and was inserted into the multiple cloning site of the pEGFP-N1 vector, upstream of the GFP coding sequence. In order to delete the αIIb stop codon and to fuse the 3′ end of αIIb in frame to the coding sequence of GFP, a cassette was generated by PCR using pcDNA3.1/Zeo(−)αIIb as a template and the following primers. The sense primer corresponded to nucleotides 2703–2731 of αIIb with a *Bam*HI restriction site (5′-GCCCTCGAGGCTTCAGGATCCAGTTC-3′), and the antisense primer corresponded to nucleotides 3097–3123 with an *Age*I restriction site (5′-ACCGGTATCTCCCCC-TCTTCATCATCTTCTTCCAG-3′). The PCR-amplified cassette was inserted into the pEGFP-N1-αIIb vector, from which the corresponding sequence had been excised by *Bam*HI and *Age*I digestion. A similar approach was also used to generate the $\beta 3_{GFP}$ expression vector. Briefly, the full-length β3 cDNA was excised from the pBJ1-β3 vector [11] and inserted into the pEGFP-N1 vector (ClonTech Laboratories). The exchange cassette was generated using the sense primer 5′-CGACCG-AAAAGAATTCGCTAAATTTG-3′ and the anti-sense primer 5′-GTCGACAAAGTGCCCCGGTACGTGATATT-3′, with *Eco*RI (5′) and *Sal*I (3′) restriction sites respectively, and was inserted into the pEGFP-N1-β3 vector to replace the corresponding wild-type (wt) sequence. The coding sequence of each vector was verified by dideoxy sequencing using the T7 sequencing kit from Amersham Pharmacia Biotech. For each chimaeric integrin subunit, GFP was separated from the C-terminal part of the integrin subunit by a spacer corresponding to five amino acids for αIIb_{GFP} (IPVAT; where single-letter amino-acid notation has been used) and to 14 amino acids for $\beta 3_{GFP}$ (LSTVPRARDPPVAT). All the oligonucleotides used for PCR amplification and sequencing reactions were purchased from Life Technologies (Merelbeke, Belgium) or Eurogentec (Seraing, Belgium).

CHO cell transfection

CHO cell clones, previously described by us and expressing either recombinant human αIIb or β3 [12], were transfected with the complementary β3wt, $\beta 3_{GFP}$ or αIIb_{GFP} vectors using LIPOFECTAMINE™ (Life Technologies), in order to generate the following cell clones: CHO αIIbβ3wt, CHO $\alpha IIb_{GFP}\beta 3$ and CHO $\alpha IIb\beta 3_{GFP}$. Stably transfected cells were obtained by growth in neomycin selection medium (0.7 mg/ml) and were analysed by flow cytometry for autofluorescence and cell surface expression of the transfected integrin. CHO cells expressing wt αIIbβ3 were further transfected with pEGFP-N1 encoding free GFP and stable cell clones were selected.

Flow cytometry and capping experiments

Transfected cells were detached, washed and incubated in Iscove's modified Dulbecco's medium (IMDM; 5×10^5 cells/100 μl) in the presence of anti-β3 mAbs as previously described [11]. Capping experiments were performed by incubating the cells either at 37 °C (antigen capping) or at 4 °C (control) with the primary anti-β3 mAb P37, followed by secondary unlabelled anti-mouse IgG. The cells were then washed, fixed with methanol on a glass coverslip, mounted in PBS/glycerol and micro-photographed. For mAb PAC1 binding studies to activated αIIbβ3, 5×10^5 cells in 50 μl of IMDM were preincubated for 20 min at 20 °C in the presence or absence of the activating mAb D3 (3 μg). For some experiments, non-specific binding of mAb PAC1 was determined by incubating the cells for 20 min at 20 °C in the presence or absence of 1 mM RGDS. mAb PAC1 (3.5 μg diluted in 50 μl of IMDM) was then directly added to the suspension and the cells were further incubated for 45 min at 20 °C. The cells were then washed with cold IMDM and incubated for 30 min on ice with R-phycoerythrin-conjugated anti-mouse IgM diluted in IMDM, washed and finally resuspended in 200 μl of PBS containing 1 mg/ml D-glucose and 2 μg/ml 7-AAD. The cells were analysed on an Epics Elite ESP flow cytometer (Coulter Electronics, Hialeah, FL, U.S.A.). After electronic compensation of the FL1, FL2 and FL4 fluorescence channels, PAC1 binding (FL2) was analysed on living cells (7-AAD negative cells in FL4) expressing GFP (FL1).

Western-blot analysis

Transfected CHO cells were lysed for 30 min at 4 °C in lysis buffer containing 10 mM Tris/HCl (pH 7.4), 150 mM NaCl, 1 % (v/v) Triton X-100 and protease inhibitors (1.5 μM pepstatin A,

4 μM leupeptin, 28 μM E64 and 0.5 mM pefabloc). Protein samples (50 μg) were resolved by SDS/PAGE, transferred on to nitrocellulose and processed as previously described [11]. Adhesion-dependent p125^{FAK} phosphorylation was assayed as previously described [12]. Briefly, freshly harvested cells were plated on Petri dishes pre-coated with 100 μg/ml fibrinogen and were allowed to spread for 2 h. The cells were then lysed *in situ* and p125^{FAK} was immunoprecipitated and analysed by Western blotting. The blots were developed using enhanced chemiluminescence (Pierce, Rockford, IL, U.S.A.) according to the manufacturer's instructions.

Cell adhesion inhibition assay

The cell adhesion inhibition assay was carried out as previously described [11]. Briefly, 96-well microtitre plates were coated overnight at 4 °C with 20 μg/ml fibrinogen or fibronectin diluted in IMDM. Washed cells (3×10^5/ml) were preincubated for 20 min at 20 °C with blocking anti-αIIbβ3, anti-αvβ3 or anti-α5β1 mAbs, or control non-immune IgG. The cells (100 μl) were plated on the microtitre plates, allowed to spread for 40 min at 37 °C and finally microphotographed. The percentage of spread and round cells was determined as previously described [11].

Immunofluorescence staining of focal adhesion plaques

Glass coverslips were coated overnight at 4 °C with 20 μg/ml fibrinogen diluted in IMDM. Cells were harvested, washed, plated on the glass coverslips and allowed to spread for 3 h. The cells were then fixed and treated with primary and secondary antibodies as previously described [12]. Coverslips were mounted in Mowiol 40-88/1,4-diazadicyclo[2.2.2]octane (DABCO) (Sigma) and microphotographs were taken using a 63× oil immersion objective and Ilford HP5 films (Ilford, Mobberley, U.K.).

Cell aggregation

Cell aggregation assays were performed according to Lyman et al. [13]. Briefly, washed cells were resuspended at 2×10^7/ml in Tyrode's buffer (137 mM NaCl, 2.8 mM KCl, 12 mM $NaHCO_3$, 5.5 mM glucose, 0.4 mM NaH_2PO_4 and 10 mM Hepes, pH 7.4) containing 3.5 mg/ml BSA, and treated with either 10 mM dithiothreitol (DTT) or Tyrode's buffer for 20 min at 20 °C as previously described [14,15]. The cells were then washed and resuspended in Tyrode's buffer. Aggregation was performed in a 24-well plate following the addition to each well of 250 μl of cell suspension, 33 μl of 2 mg/ml fibrinogen or Tyrode's buffer, and 20 μl of 15 mM $CaCl_2$. The plates were rotated on a shaker for 20 min at 80 rev./min. The cell suspensions were then fixed with 0.25% paraformaldehyde, mounted on a slide and immediately microphotographed.

Video microscopy

Cells were plated on fibrinogen-coated glass coverslips and observed in an open chamber at 37 °C, 7% CO_2, on an inverted microscope (Leica DMIRBE) equipped for epifluorescence and phase-contrast microscopy. Data were acquired with a cooled CCD Micromax camera (Princeton Instruments, Evry, France) driven by Metamorph software and stored as 16-bit digital images. Phase contrast and fluorescent images were taken every 30 s. The video sequences were analysed and processed using Metamorph software.

RESULTS AND DISCUSSION

Surface expression of recombinant αIIbβ3$_{GFP}$ and αIIb$_{GFP}$β3 in CHO cells

To test whether a functional autofluorescent αIIbβ3 receptor could be expressed in heterologous cells, allowing direct

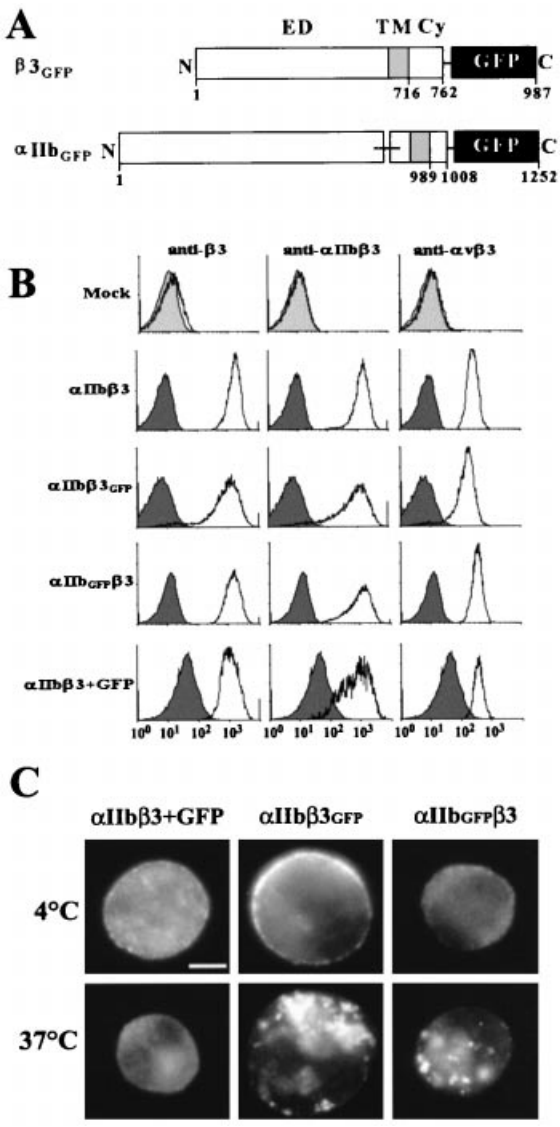

Figure 1 Expression of GFP-tagged αIIbβ3 integrins in CHO cells

(**A**) Representation of the structural organization of the αIIb$_{GFP}$ and β3$_{GFP}$ chimaeras. The GFP moiety is fused to the carboxy terminus of each subunit with an in-frame spacer of five amino acids for αIIb$_{GFP}$ and 14 amino acids for β3$_{GFP}$. The position and size (in amino acids) of the different structural domains (not drawn to scale) are indicated. ED, extracellular domain; TM, transmembrane domain; Cy, cytoplasmic tail; GFP, GFP tag. (**B**) Cell surface expression of GFP-tagged β3 integrins. Cell surface expression of native and GFP-tagged β3 integrins was measured by flow cytometry. β3 integrin labelling was performed using mAbs P37 (anti-β3), PI2-46 (complex-specific anti-αIIbβ3) and 23C6 [complex-specific anti-(human αvβ3), also cross-reacting with αv$_{(hamster)}$β3$_{(human)}$]. The cells were first labelled with the specific mAb, then with R-phycoerythrin-conjugated goat anti-mouse IgG. The shaded areas represent background fluorescence (secondary antibody alone). (**C**) Antibody-mediated capping of αIIbβ3. Transfected CHO cells were incubated with primary anti-β3 mAb P37 and secondary unlabelled anti-mouse IgG for 45 min each at either 4 °C, for control cell surface labelling, or 37 °C, for antibody-mediated capping. After washing, the cells were fixed on a glass coverslip, mounted in PBS/glycerol and microphotographed. Bar = 10 μm.

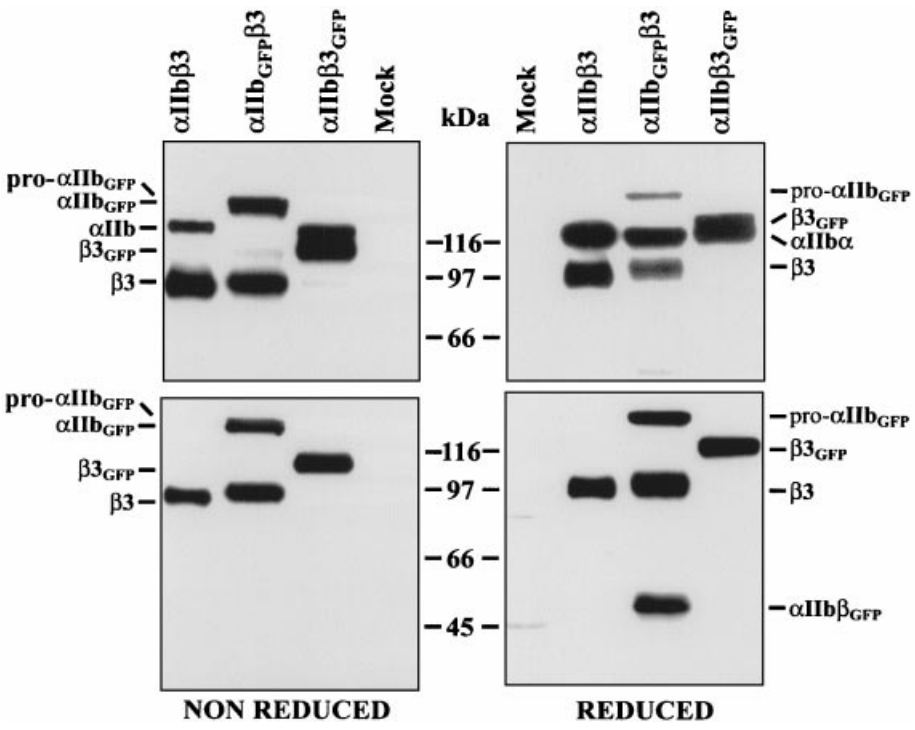

Figure 2 Immunochemical analysis of αIIb_{GFP} and $\beta 3_{GFP}$ expressed in CHO cells

Upper panels: samples (50 μg of protein) of CHO cell lysates were electrophoresed on a 7.5% (w/v) acrylamide gel under non-reducing and reducing conditions, transferred on to nitrocellulose and probed with mAbs S1.3 [anti-(αIIb heavy chain)] and 4D10G3 (anti-β3). Lower panels: the blots were then stripped and reprobed with a mixture of anti-β3 (P37) and anti-GFP antibodies.

observation of integrins in living cells, we generated cDNA constructs encoding αIIb or β3 with GFP fused to the C-terminal cytoplasmic tail (Figure 1A). These αIIb or β3 constructs were stably transfected into established CHO cell clones expressing the complementary recombinant wt α or β subunit, and transfected cells were selected for similar fluorescence intensities. As a control, αIIbβ3-expressing CHO cells were also transfected with a plasmid encoding solely free GFP. Surface expression of the recombinant GFP-tagged αIIbβ3 integrins was monitored by flow cytometry based on two criteria: GFP autofluorescence of the cells, as well as indirect immunofluorescence labelling using anti-β3, anti-αIIbβ3 and anti-αvβ3 primary mAbs and R-phycoerythrin-conjugated secondary antibodies. As shown in Figure 1(B), surface labelling of cells expressing either wt β3, GFP-tagged αIIb or GFP-tagged β3 subunits revealed similar immunofluorescence intensities, providing evidence that the GFP-tagged αIIb or β3 polypeptides were correctly processed and reached the cell surface as heterodimers. Since the CHO cells used in the present study express endogenous αvβ1 and αvβ5, but are devoid of αvβ3, transfection of the human $\beta 3_{GFP}$ subunit into these cells also induced the expression of chimaeric $\alpha v_{(hamster)}\beta 3_{GFP}$ receptors, although $\alpha v_{(hamster)}\beta 3_{GFP}$ expression was markedly reduced compared with $\alpha IIb\beta 3_{GFP}$, most probably due to the lower endogenous pool of hamster αv. Transfection of GFP cDNA alone into αIIbβ3-expressing CHO cells allowed the expression of high levels of free GFP. However, as shown in Figure 1(C), direct microscopic observation of the autofluorescent cells in suspension following antibody-induced αIIbβ3 capping at 37 °C revealed diffuse intracellular fluorescence in these cells. In contrast, cells expressing GFP-tagged αIIbβ3 exhibited an intense autofluorescent cap corresponding to unlabelled, immunoclustered αIIbβ3, with a complete disappearance of the diffuse fluorescence staining observed when the same cells were kept at 4 °C (Figure 1C). The colocalization of autofluorescent GFP with antibody-clustered αIIbβ3 clearly demonstrates that the GFP-tagged αIIbβ3 receptors were essentially intact and did not undergo proteolytic cleavage causing the release of the GFP moiety.

Immunochemical analysis of $\beta 3_{GFP}$ and αIIb_{GFP} in CHO cells

Immunochemical analysis of $\alpha IIb\beta 3_{GFP}$ and $\alpha IIb_{GFP}\beta 3$ expressed in CHO cells was performed by Western-blot analysis. As shown in Figure 2, under non-reducing conditions, both αIIb_{GFP} and $\beta 3_{GFP}$ exhibited a decreased electrophoretic mobility compared with platelet αIIb and β3, with the high-molecular-mass doublet (not clearly resolved) corresponding to pro-αIIb_{GFP} and mature αIIb_{GFP}. Following disulphide bond reduction, $\beta 3_{GFP}$ exhibited the typical decreased electrophoretic mobility, also observed for wt β3, while mature αIIb_{GFP} resolved into its αIIbα heavy chain, visualized with an anti-αIIb antibody (upper panel) and $\alpha IIb\beta_{GFP}$ light chain, visualized with an anti-GFP antibody (lower panel). No change in the electrophoretic mobility of the uncleaved pro-αIIb_{GFP} was observed. The difference in the labelling intensity of pro-αIIb_{GFP} shown in the upper and lower panels was due to the use of two different antibodies (monoclonal anti-αIIb and polyclonal anti-GFP respectively). No band corresponding to free GFP was detected, indicating that the αIIb_{GFP} and $\beta 3_{GFP}$ fusion proteins are intact in the living cell and that GFP is not spontaneously released from the integrin subunit cytoplasmic tail through proteolytic cleavage.

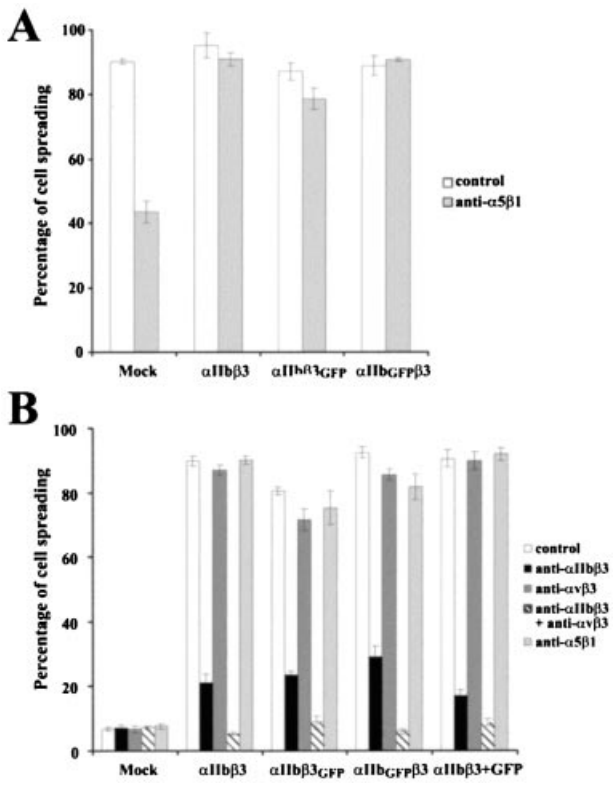

Figure 3 Inhibition of transfected CHO cell adhesion to immobilized fibrinogen

(**A**) Cell adhesion assay on fibronectin. Transfected CHO cells were seeded on microtitre plates coated with 20 μg/ml fibronectin. The cells were allowed to adhere for 40 min in the presence of either non-immune control IgG (white bars) or the blocking anti-$\alpha5\beta1$ mAb PB1 (light-grey bars). The cells were then microphotographed and the percentages of spread and round cells were determined. The results are presented as the means $\pm$ S.D. of three independent experiments performed in triplicate. (**B**) Inhibition of cell spreading to immobilized fibrinogen. Cells were seeded on fibrinogen-coated microtitre plates. The cells were allowed to adhere for 40 min in the presence of non-immune control IgG (white bars), the blocking anti-αIIb$\beta3$ mAb PI2-46 (black bars), the blocking anti-$\alpha v\beta3$ mAb LM609 (dark-grey bars), a mixture of PI2-46 and LM609 (hatched bars) or the blocking anti-$\alpha5\beta1$ mAb PB1 (light-grey bars). Quantification of cell spreading was performed as described above.

Subcellular localization of αIIb$\beta3_{GFP}$ and $\alpha IIb_{GFP}\beta3$ during cell spreading and involvement in outside-in signalling

Integrin–cytoskeleton interactions are known to rely essentially on a structurally intact integrin β subunit, since the β subunit cytoplasmic tail by itself contains sufficient information to target integrins to focal adhesion plaques and to trigger tyrosine phosphorylation of intracellular proteins [16,17]. Also, integrin β subunit splice variants with an alternative cytoplasmic tail [18], cytoplasmic tail deletion mutants [12,19] or a naturally occuring point mutation in the cytoplasmic tail of $\beta3$ [20] have all been reported to prevent cell spreading, fibrin clot retraction and integrin-dependent signalling. With the fusion of GFP to the cytoplasmic tail of the $\beta3$ subunit, we expected that the relatively large size of GFP (approx. 27 kDa) would interfere with $\beta3$ integrin–cytoskeleton interactions, as well as receptor signalling, with $\beta3_{GFP}$ acting as a dominant negative subunit. To our surprise, however, fibrinogen-dependent cell spreading of CHO cells expressing $\alpha IIb_{GFP}\beta3$ or $\alpha IIb\beta3_{GFP}$ was essentially identical with that mediated by native αIIb$\beta3$ (Figure 3). This spreading could not be attributed solely to the chimaeric $\alpha v_{(hamster)}\beta3_{(human)}$ receptor, since the blocking anti-$\alpha v\beta3$ mAb LM609 had no inhibitory effect, while spreading was reduced to 30 % with the anti-αIIb$\beta3$ mAb PI2-46 (Figure 3B). However, incubation of the cells with LM609 and PI2-46 blocked cell spreading by 90 %. Since fibrinogen has been shown to be a ligand for Mn^{2+}-activated $\alpha5\beta1$ [21], and to exclude the potential involvement of endogenous $\alpha5\beta1$ in CHO transfectant cell adhesion to immobilized fibrinogen, we tested the effect of the hamster-specific and blocking anti-$\alpha5\beta1$ mAb PB1 [22] on CHO cell adhesion. As shown in Figure 3(A), mAb PB1 blocked mock-transfected CHO cell spreading on fibronectin by 60 %, but had no inhibitory effect on fibrinogen-dependent cell spreading, indicating that the spreading of our CHO transfectants on fibrinogen is exclusively mediated by overexpressed $\beta3$ integrins.

Analysis of GFP-tagged αIIb$\beta3$ translocation to focal adhesions following cell spreading on fibrinogen revealed that the green autofluorescence of $\alpha IIb\beta3_{GFP}$ overlapped with the indirect immunofluorescent red labelling of αIIb$\beta3$ (Figure 4A), and was localized in focal contacts at the tips of rhodamine-labelled stress fibres, as demonstrated with an anti-GFP antibody (Figure 4B). In contrast, in cells expressing free GFP, a strong autofluorescence was observed in the nucleus and to a lesser extent in the cytoplasm, without any colocalization of GFP with immunolabelled αIIb$\beta3$ (Figure 4A) or stress fibres (Figure 4B). Interestingly, in cells expressing $\alpha IIb_{GFP}\beta3$, autofluorescence was observed in focal adhesions, as well as around the nucleus. This perinuclear staining could correspond to incompletely processed pro-αIIb_{GFP} retained in the endoplasmic reticulum.

FAK tyrosine phosphorylation is one of the early post-ligand-binding events mediated by integrins, and relies essentially on a functional β subunit cytoplasmic tail [23,24]. To explore the outside-in signalling potential of GFP-tagged αIIb$\beta3$, $p125^{FAK}$ tyrosine phosphorylation was assessed during cell spreading. Cells plated on fibrinogen-coated Petri dishes were allowed to spread for 2 h at 37 °C and then lysed *in situ*; $p125^{FAK}$ was immunoprecipitated and analysed for tyrosine phosphorylation by Western-blot analysis. As shown in Figure 5, integrin-dependent $p125^{FAK}$ phosphorylation was detected in $\alpha IIb_{GFP}\beta3$- and $\alpha IIb\beta3_{GFP}$-expressing cells to a similar extent as that observed for wt αIIb$\beta3$. In contrast, only background phosphorylation was seen when cells were kept in suspension or when mock-transfected cells were plated on fibrinogen. This $p125^{FAK}$ phosphorylation could not be attributed to endogenous $\alpha5\beta1$ engagement, since the blocking mAb PB1 had no inhibitory effect on CHO transfectant cell spreading (Figure 3). These results therefore demonstrate that fusion of GFP to the cytoplasmic tail of either the αIIb or $\beta3$ integrin subunit does not interfere with integrin-mediated $p125^{FAK}$ tyrosine phosphorylation.

GFP tagged to the cytoplasmic tail of $\beta3$, but not to αIIb, induces spontaneous CHO cell aggregation in the presence of soluble fibrinogen

Although integrin cytoplasmic tails play an important role in regulating integrin affinity, the precise functional role of each subunit in this process remains unclear [7]. With the use of the two-hybrid system, a number of intracellular proteins have been identified that interact with integrin α or β cytoplasmic tails [10]. Interestingly, only proteins interacting with integrin β subunits have so far been shown to modulate integrin affinity [25–27]. Among these, $\beta3$-endonexin, which selectively interacts with $\beta3$, is of particular interest, since overexpression of $\beta3$-endonexin in αIIb$\beta3$-expressing CHO cells causes increased fibrinogen binding and fibrinogen-dependent cell aggregation [26]. To study the

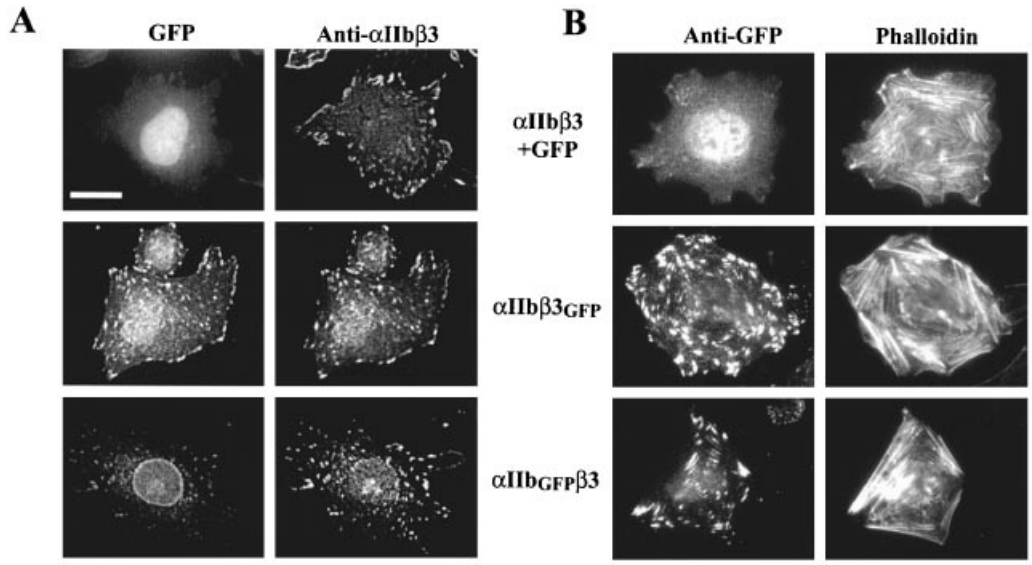

Figure 4 Subcellular localization of GFP-tagged αIIbβ3 integrins in CHO cells plated on fibrinogen

Cells were allowed to spread for 3 h on fibrinogen-coated glass coverslips. The cells were subsequently fixed and stained with anti-αIIbβ3 mAb PI2-73, followed by staining with rhodamine-labelled secondary anti-mouse IgG (**A**), or with anti-GFP polyclonal antibody, followed by staining with FITC-labelled secondary anti-rabbit IgG and rhodamine-labelled phalloidin (**B**). The glass coverslips were mounted in Mowiol/DABCO and microphotographed. The same cell is shown: GFP autofluorescence and αIIbβ3 immunofluorescent labelling (**A**); GFP labelling and stress fibre staining (**B**). Bar = 10 μm.

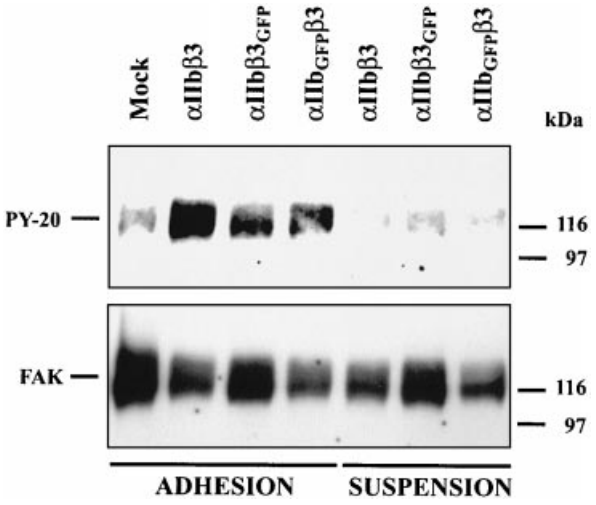

Figure 5 GFP-tagged αIIbβ3 integrins mediate tyrosine phosphorylation of p125^{FAK}

For αIIb$_{GFP}\beta$3- and αIIb$\beta3_{GFP}$-dependent p125^{FAK} tyrosine phosphorylation, adherent cells plated on fibrinogen were lysed *in situ* and p125^{FAK} was immunoprecipitated using a polyclonal anti-FAK antibody. The precipitates were resolved by SDS/PAGE and transferred on to nitrocellulose. The membrane was first probed with the anti-phosphotyrosine mAb PY-20 (upper panel), then stripped and reprobed with the anti-FAK mAb (lower panel).

effect of the GFP tag on αIIbβ3 affinity modulation, we compared the ligand binding capacity of GFP-tagged αIIbβ3 with that of wt αIIbβ3, using either DTT treatment of the cells or the activating mAb D3 for αIIbβ3 stimulation. Surprisingly, in the absence of any stimulation, αIIb$\beta3_{GFP}$-expressing CHO cells spontaneously aggregated when brought into contact with soluble fibrinogen, in contrast with the cells expressing αIIb$_{GFP}\beta$3 or wt αIIbβ3, that only aggregated following DTT treatment (Figure 6A). In the absence of DTT, fibrinogen-dependent aggregation of αIIb$\beta3_{GFP}$-expressing CHO cells could be completely inhibited by RGDS or the blocking anti-αIIbβ3 mAb PI2-46 (results not shown), demonstrating the direct involvement of αIIb$\beta3_{GFP}$ in this process. To confirm further that αIIb$\beta3_{GFP}$ was able to interact with fibrinogen in the absence of receptor activation, flow cytometry analysis was performed using mAb PAC1 as a fibrinogen mimetic. As shown in Figure 6(B), PAC1 bound spontaneously to αIIb$\beta3_{GFP}$-expressing cells, and this binding could be specifically inhibited by RGDS, whereas PAC1 did not interact with αIIb$_{GFP}\beta$3-expressing cells. Following stimulation of the cells with the activating antibody D3, increased PAC1 binding was observed for αIIb$\beta3_{GFP}$-expressing cells, similar to that seen for αIIb$_{GFP}\beta$3-expressing cells, demonstrating that not all αIIb$\beta3_{GFP}$ receptors were in an active conformation, a result also reported following overexpression of β3-endonexin [26] or the head domain of talin [27] in αIIbβ3-positive CHO cells. Although we have no explanation for this partial αIIbβ3 receptor activation, our results provide further evidence that a structural modification of the intact cytoplasmic tail of the β3 integrin subunit, rather than the αIIb subunit, plays a pivotal role in αIIbβ3 activation. Indeed, as shown by Hato et al. [28], a structural modification of the integrin αIIb cytoplasmic tail did not modify the affinity state of αIIbβ3. Taken together, our data suggest that the structural modification of the β3 cytoplasmic tail, necessary for the exposure of the high-affinity ligand-binding pocket on αIIbβ3, can be brought about not only by specific intracellular proteins, such as β3-endonexin [26], or cytoskeletal proteins, such as talin [27], but also by non-specific macromolecules, as shown in the present study for GFP.

Dynamic redistribution of αIIbβ3 during cell attachment

Using time-lapse imaging, we monitored the dynamics of GFP-tagged αIIbβ3 integrin redistribution during the early events of

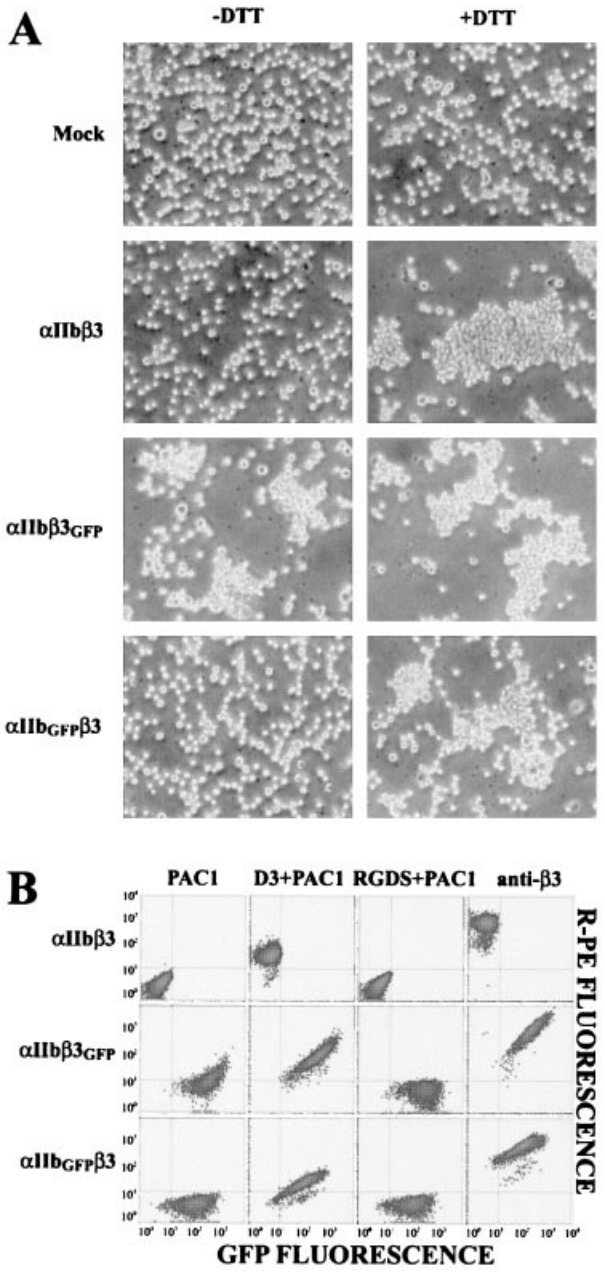

Figure 6 Analysis of the affinity state of the GFP-tagged αIIbβ3 integrins expressed in CHO cells

(**A**) CHO cell aggregation in the presence of soluble fibrinogen. Transfected cells were harvested, resuspended in Tyrode's buffer and treated with 10 mM DTT or buffer for 20 min at 20 °C. After washing, fibrinogen and $CaCl_2$ were added and the cell suspension was rotated on a shaker for 20 min at 80 rev./min. The cells were then fixed, mounted on slides and immediately microphotographed. The data are representative of three independent experiments. (**B**) Flow cytometry analysis of PAC1 binding. CHO cells expressing the indicated integrins were analysed for PAC1 binding using R-phycoerythrin (R-PE)-conjugated anti-IgM as second layer antibody (*y*-axis). Green-fluorescent cells are plotted on the *x*-axis. Each contour plot represents 10 000 cells. Maximal PAC1 binding was achieved in the presence of the activating mAb D3, whereas non-specific PAC1 binding was examined in the presence of 1 mM RGDS. Anti-β3 mAb labelling illustrates β3 integrin expression on the cell surface.

cell attachment, by focusing on the autofluorescent integrin receptors located at the cell–substrate interface. αIIb$\beta3_{GFP}$-transfected cells were plated on fibrinogen-coated coverslips mounted on the microscope stage and images were acquired every 30 s over a period of 60 min. As shown in Figure 7, during the very early events of the cell contact with the substratum, clustering of integrins at the rim of the cell contact area was observed. With the time-dependent increase in cell attachment, this autofluorescent circular rim increased in diameter, visualizing the limit of the cell contact area, to finally overlap with the boundary of the attached cell. With the appearance of the first cell protrusions initiating cell spreading, the autofluorescent rim disintegrated and a reorganization of integrins into small focal complexes was observed, which grew in size to become well-established focal adhesion plaques, localized preferentially at sites of high tension, such as microspikes (Figure 7). Similar results were also obtained with CHO cells expressing $\alpha IIb_{GFP}\beta3$ (results not shown). These data demonstrate that fully functional autofluorescent β3 integrins can be expressed and visualized in living cells, providing a powerful tool to study the dynamics of integrin functions in transgenic animals in various normal and pathological conditions.

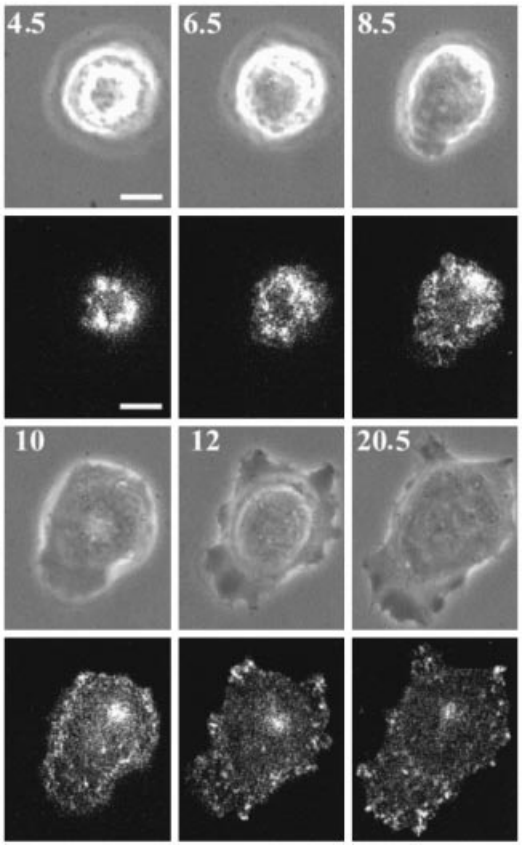

Figure 7 Dynamic distribution of GFP-tagged αIIbβ3 integrins during cell spreading

CHO cells expressing αIIb$\beta3_{GFP}$ were washed twice, harvested and plated on a coverslip coated with 20 μg/ml fibrinogen. The coverslip was then placed in an open chamber at 37 °C mounted on the video microscope stage. Immediately after plating, images at the focal plane of the coverslip (cell–substrate interface) were acquired every 30 s for a period of 60 min. Phase-contrast and fluorescence images were acquired to correlate cell shape and αIIbβ3 integrin distribution. Indicated numbers represent time points given in min. Bar = 10 μm. A video of this Figure can be viewed at http://www.BiochemJ.org/bj/357/bj3570529add.htm.

We thank Drs J. Gonzalez-Rodriguez, M. Horton, C. Kaplan, L. Jennings and D. Phillips for their generous gifts of monoclonal antibodies. We are also grateful to

J.-B. Sibarita and J. Fradelizi (Digital Imaging Service, UMR144/CNRS, Institut Curie, Paris) for helpful assistance with time-lapse imaging analysis, and W. Ammerlaan (Immunology Department, Laboratoire National de Santé, Luxembourg) for assistance with flow cytometry analysis. This work was supported by grants from the Centre de Recherche Public-Santé (CRP-Santé; Luxembourg), the Centre National de la Recherche Scientifique (CNRS; France), the Fondation Luxembourgeoise Contre le Cancer (Luxembourg), and the EC Biomed Project Grant BMH4-CT98-3517. S.P. is a recipient of a fellowship from the Ministère de la Culture, de l'Enseignement Supérieur et de la Recherche, Luxembourg. The data presented were obtained as part of a doctoral thesis to be submitted by S.P. to the University Paris VII. M.C.M.-K. is a recipient of an EC Marie Curie fellowship (ERBFMBI-CT96-1531).

REFERENCES

1 Chalfie, M., Tu, Y., Euskirchen, G., Ward, W. W. and Prasher, D. C. (1994) Green fluorescent protein as a marker for gene expression. Science (Washington, D.C.) **263**, 802–805
2 Tsien, R. Y. (1998) The green fluorescent protein. Annu. Rev. Biochem. **67**, 509–544
3 Adams, C. L., Chen, Y. T., Smith, S. J. and Nelson, W. J. (1998) Mechanisms of epithelial cell-cell adhesion and cell compaction revealed by high-resolution tracking of E-cadherin-green fluorescent protein. J. Cell Biol. **142**, 1105–1119
4 Eppenberger, H. M. and Zuppinger, C. (1999) In vitro reestablishment of cell-cell contacts in adult rat cardiomyocytes. Functional role of transmembrane components in the formation of new intercalated disk-like cell contacts. FASEB J. **13**, S83–S89
5 Fabbri, M., Fumagalli, L., Bossi, G., Bianchi, E., Bender, J. R. and Pardi, R. (1999) A tyrosine-based sorting signal in the β2 integrin cytoplasmic domain mediates its recycling to the plasma membrane and is required for ligand-supported migration. EMBO J. **18**, 4915–4925
6 Smilenov, L. B., Mikhailov, A., Pelham, R. J., Marcantonio, E. E. and Gundersen, G. G. (1999) Focal adhesion motility revealed in stationary fibroblasts. Science (Washington, D.C.) **286**, 1172–1174
7 Parise, L. V. (1999) Integrin αIIbβ3 signaling in platelet adhesion and aggregation. Curr. Opin. Cell Biol. **11**, 597–601
8 Bazzoni, G. and Hemler, M. E. (1998) Are changes in integrin affinity and conformation overemphasized? Trends Biochem. Sci. **23**, 30–34
9 van Willigen, G. and Akkerman, J. W. N. (1997) Phosphorylation reactions and the affinity state of platelet integrin αIIbβ3. Platelets **8**, 225–234
10 Hughes, P. E. and Pfaff, M. (1998) Integrin affinity modulation. Trends Cell Biol. **8**, 359–364
11 Kieffer, N., Melchior, C., Guinet, J. M., Michels, S., Gouon, V. and Bron, N. (1996) Serine 752 in the cytoplasmic domain of the β3 integrin subunit is not required for $\alpha v\beta$3 postreceptor signaling events. Cell Adhes. Commun. **4**, 25–39
12 Schaffner-Reckinger, E., Gouon, V., Melchior, C., Plançon, S. and Kieffer, N. (1998) Distinct involvement of β3 integrin cytoplasmic domain tyrosine residues 747 and 759 in integrin-mediated cytoskeletal assembly and phosphotyrosine signaling. J. Biol. Chem. **273**, 12623–12632
13 Lyman, S., Gilmore, A., Burridge, K., Gidwitz, S. and White, G. C. (1997) Integrin-mediated activation of focal adhesion kinase is independent of focal adhesion formation or integrin activation – Studies with activated and inhibitory β3 cytoplasmic domain mutants. J. Biol. Chem. **272**, 22538–22547
14 Zucker, M. B. and Masiello, N. C. (1984) Platelet aggregation caused by dithiothreitol. Thromb. Haemostasis **51**, 119–124
15 Kouns, W. C., Jutzi, J., Jennings, L. K. and Steiner, B. (1993) Disulfide reduction "activates" integrin αIIbβ3 (GPIIb-IIIa). Thromb. Haemostasis **69**, 785–791
16 Ylänne, J., Chen, Y., O'Toole, T. E., Loftus, J. C., Takada, Y. and Ginsberg, M. H. (1993) Distinct functions of integrin α and β subunit cytoplasmic domains in cell spreading and formation of focal adhesions. J. Cell Biol. **122**, 223–233
17 LaFlamme, S. E., Thomas, L. A., Yamada, S. S. and Yamada, K. M. (1994) Single subunit chimeric integrins as mimics and inhibitors of endogenous integrin functions in receptor localization, cell spreading and migration, and matrix assembly. J. Cell Biol. **126**, 1287–1298
18 van Kuppevelt, T. H., Languino, L. R., Gailit, J. O., Suzuki, S. and Ruoslahti, E. (1989) An alternative cytoplasmic domain of the integrin β3 subunit. Proc. Natl. Acad. Sci. U.S.A. **86**, 5415–5418
19 Wang, R. G., Shattil, S. J., Ambruso, D. R. and Newman, P. J. (1997) Truncation of the cytoplasmic domain of β3 in a variant form of Glanzmann thrombasthenia abrogates signaling through the integrin αIIbβ3 complex. J. Clin. Invest. **100**, 2393–2403
20 Chen, Y. P., O'Toole, T. E., Ylänne, J., Rosa, J. P. and Ginsberg, M. H. (1994) A point mutation in the integrin β3 cytoplasmic domain (S752–P) impairs bidirectional signaling through αIIbβ3 (platelet glycoprotein IIb-IIIa). Blood **84**, 1857–1865
21 Suehiro, K., Gailit, J. and Plow, E. F. (1997) Fibrinogen is a ligand for integrin $\alpha 5\beta 1$ on endothelial cells. J. Biol. Chem. **272**, 5360–5366
22 Brown, P. J. and Juliano, R. L. (1985) Selective inhibition of fibronectin-mediated cell adhesion by monoclonal antibodies to a cell-surface glycoprotein. Science (Washington, D.C.) **228**, 1448–1451
23 Akiyama, S. K., Yamada, S. S., Yamada, K. M. and LaFlamme, S. E. (1994) Transmembrane signal transduction by integrin cytoplasmic domains expressed in single-subunit chimeras. J. Biol. Chem. **269**, 15961–15964
24 Clark, E. A. and Brugge, J. S. (1995) Integrins and signal transduction pathways: the road taken. Science (Washington, D.C.) **268**, 233–239
25 Kolanus, W., Nagel, W., Schiller, B., Zeitlmann, L., Godar, S., Stockinger, H. and Seed, B. (1996) αLβ2 integrin/LFA-1 binding to ICAM-1 induced by cytohesin-1, a cytoplasmic regulatory molecule. Cell (Cambridge, Mass.) **86**, 233–242
26 Kashiwagi, H., Schwartz, M. A., Eigenthaler, M., Davis, K. A., Ginsberg, M. H. and Shattil, S. J. (1997) Affinity modulation of platelet integrin αIIbβ3 by β3-endonexin, a selective binding partner of the β3 integrin cytoplasmic tail. J. Cell Biol. **137**, 1433–1443
27 Calderwood, D. A., Zent, R., Grant, R., Rees, D. J. G., Hynes, R. O. and Ginsberg, M. H. (1999) The talin head domain binds to integrin β subunit cytoplasmic tails and regulates integrin activation. J. Biol. Chem. **274**, 28071–28074
28 Hato, T., Pampori, N. and Shattil, S. J. (1998) Complementary roles for receptor clustering and conformational change in the adhesive and signaling functions of integrin αIIbβ3. J. Cell Biol. **141**, 1685–1695

Received 17 October 2000/21 March 2001; accepted 1 May 2001